Generation and manipulation of monodispersed ferrofluid emulsions : the effect of a uniform magnetic field in flow-focusing and T-junction configurations

Tan, Say-Hwa; Nguyen, Nam-Trung

2011

Tan, S. H., & Nguyen, N. T. (2011). Generation and Manipulation of Monodispersed Ferrofluid Emulsions : the Effect of an Uniform Magnetic Field in Flow-focusing and T-junction Configurations. Physical review E, 84(3).

https://hdl.handle.net/10356/94556

Generation and manipulation of monodispersed ferrofluid emulsions: The effect of a uniform magnetic field in flow-focusing and T-junction configurations

Say Hwa Tan and Nam-Trung Nguyen*

School of Mechanical and Aerospace Engineering, Nanyang Technological University, 50 Nanyang Avenue, Singapore 639798, Singapore

(Received 9 February 2011; revised manuscript received 12 July 2011; published 21 September 2011)

This paper demonstrates the use of magnetically controlled microfluidic devices to produce monodispersed ferrofluid emulsions. By applying a uniform magnetic field on flow-focusing and T-junction configurations, the size of the ferrofluid emulsions can be actively controlled. The influences of the flow rates, the orientation, and the polarity of the magnetic field on the size of ferrofluid emulsions produced in both flow-focusing and T-junction configurations are compared and discussed.

DOI: 10.1103/PhysRevE.84.036317 PACS number(s): 47.55.df, 75.50.Mm, 47.61.Fg, 47.55.dd

I. INTRODUCTION

A ferrofluid is a class of "smart" fluids [1], which have been extensively used in a number of applications. Ferrofluids possess attractive properties such as easy magnetization and demagnetization, maintaining fluidity even when subjected to a strong magnetic field [2], high rates of heat transfer [3], and changes of viscosity in moderate magnetic fields [4]. These properties make ferrofluids very useful for engineering and biomedical applications. Engineering applications include cooling of loudspeakers [5], magnetic sealing in bearings [6], accelerometers [7], and tilt sensors for underground pipes [8]. In medical fields, ferrofluids are attractive drug carriers due to their intrinsic physical properties and their abilities to target specific locations, thereby minimizing severe side effects [9]. Common clinical applications include magnetic drug targeting [10], treatment of thrombosis [11], and tumor therapy [12]. Theoretical studies of ferrofluids include the well-known normal field instability and pattern formation [13], particle chain aggregation [14], and structural transitions in different magnetic fields [15].

Recently, ferrofluid emulsions have been attracting great interest from researchers due to their ability to discretize, isolate, react, compartmentalize, and magnetically transport samples and reagents to targeted locations. These features are suitable for many lab-on-a-chip applications. Ferrofluid emulsions integrated with microfluidic devices have applications in areas such as the production of magnetic particles [16], polymerase chain reaction [17], and micropumps [18]. The conventional approach to producing ferrofluid emulsions involves vigorous mixing of the ferrofluid with another immiscible fluid, applying several purification steps, and repeated pipetting to obtain highly monodispersed ferrofluid emulsions [19]. Another approach to produce submicron ferrofluid emulsions involves the use of a coquette mixer to shear the emulsions and subsequent sorting under a magnetic field to collect the narrowly size-distributed emulsions [16]. Both methods are often tedious, laborious, and time consuming. Understanding these predicaments, this paper presents a simple approach to produce highly monodispersed ferrofluid emulsions by using simple microfluidic devices such as the T-junction [20] and flow-focusing [21] geometries. These ubiquitous geometries have also been used by many to produce both water-in-oil [22] and oil-in-water [23] emulsions due to the ease of emulsion formation and the high uniformity in size distribution.

In our previous work, we demonstrated a method to control the production and manipulate the size of ferrofluid emulsions using a permanent magnet integrated into a microfluidic T-junction geometry [24]. However, this method does not allow pliable manipulation as it requires the permanent magnet to be placed at different locations. Several restrictions such as magnet strength and size also limit the manipulation process. Knowing these limitations, in this current work, water-in-oil ferrofluid emulsions are produced in both microfluidic T-junction and flow-focusing configurations and then compared. These highly monodispersed ferrofluid emulsions can be first generated and then also collected for further use. In addition to using conventional flow rates, this paper presents a robust and active mean to control the size of the ferrofluid emulsions. By applying a uniform magnetic field across the microfluidic devices, the size of the ferrofluid droplets produced can hence be actively manipulated easily using the magnetic field, which in turn is controlled by the applied electric current on an electromagnet. The effect of a uniform magnetic field in the different configurations, magnetic polarity, and orientation of the magnetic fields are also presented and discussed.

II. EXPERIMENT

A. Device fabrication

The microfluidic devices were fabricated using standard soft lithography [25]. First, a layout editor (Clewin, WieWeb software) was used to design the devices. Each microfluidic device has a total area of only 1 cm × 1 cm. The schematic and dimensions of both flow-focusing and T-junction configurations used in the experiments are shown in Fig. 1. Next, a master mold was fabricated using the negative SU-8 photoresist (SU8-2100, MicroChem). The thickness of the mold, which defines the rectangular channel depth, is 100 μm. PolyDiMethylSiloxane (PDMS) oligomer and crosslinking prepolymer were mixed in the ratio of 10:1 and placed in a vacuum desiccator for 1 h for degassing. The degassed PDMS mixture was then poured onto the master mold and cured in a 80 °C convection oven for 2 h. After curing, the cast PDMS was peeled from the SU-8 mold and punched using a manual puncher (Harris Uni-Core, World Precision

*mntnguyen@ntu.edu.sg

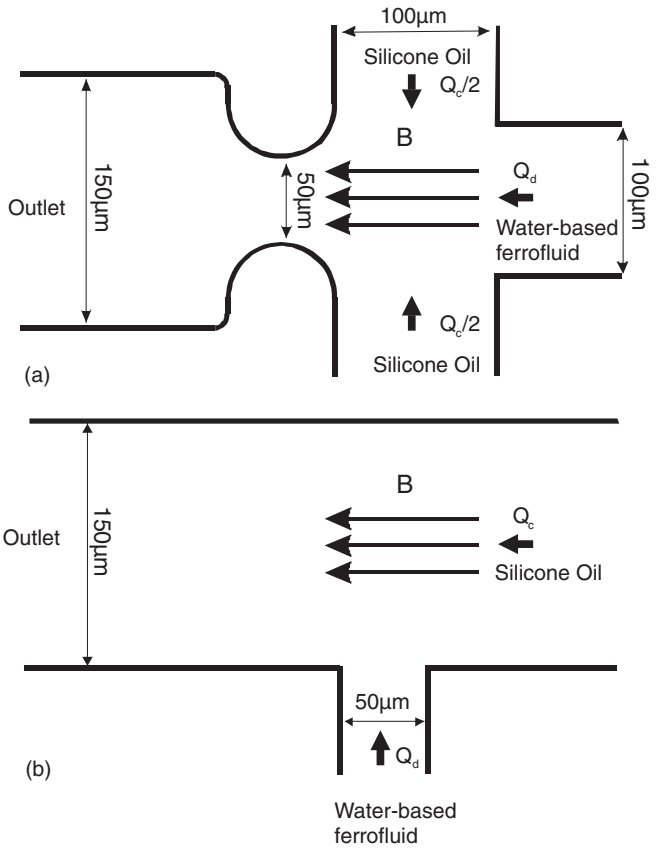

FIG. 1. Schematic of the microfluidic geometries used (not drawn to scale): (a) flow-focusing and (b) T-junction configurations. In the flow-focusing configuration, the magnetic field is aligned parallel to the dispersed phase fluid. In the T-junction configuration, the magnetic field is aligned perpendicular to the dispersed phase fluid.

Instruments). Fluidic access holes with a diameter of 1.2 mm were created. The cast PDMS was then soaked in isopropanol for 15 min followed by rinsing in distilled water. The cleaning step prevents dirt and dust from accumulating on the PDMS cast. After the cleaning process, the PDMS parts were dried using nitrogen gas at high pressure to ensure that no dust resides on the surface of the PDMS cast, which may later affect the bonding integrity. The PDMS cast was then placed in an oven at 150 °C for 30 min to ensure that the surface was free of water. Finally, oxygen plasma treatment (NT-2, BSET EQ) at 120 W for 45 s was used to bond the device to a 200-μm-layer PDMS spin coated on a glass slide. The fabrication process is summarized in Fig. 2.

B. Materials

In order to produce ferrofluid emulsions, two immiscible fluids were introduced into the inlet channels of the devices. Silicone oil (378364, Sigma-Aldrich) with a dynamic viscosity of 96 mPa s and density of 960 kg m^{-3} works as the continuous phase (CP). Water-based ferrofluid (EMG707, Ferrotec) with a dynamic viscosity of 5 mPa s and density of 1100 kg m^{-3} works as the dispersed phase (DP). The ferrofluids contain spherical Fe_3O_4 magnetic nanoparticles which have an average diameter of 10 nm. Because the size of the magnetic nanoparticles is very small, a weak or negligible magnetoviscous effect

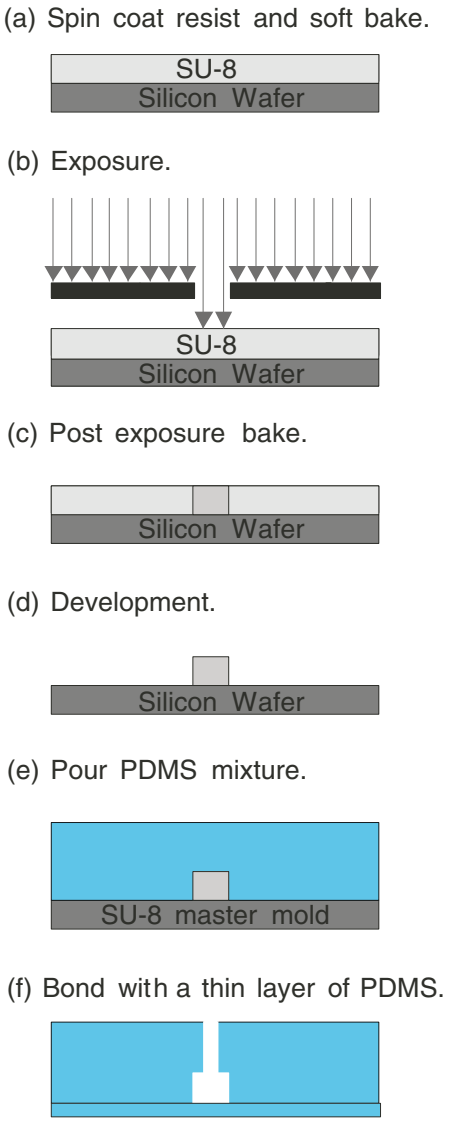

FIG. 2. (Color online) Fabrication process of the microfluidic device: (a–d) fabrication of the SU-8 master mold and (e, f) the fabrication of the PDMS device.

is expected [5]. The volume concentration of the magnetic nanoparticles is 1.8% and its initial susceptibility is 0.36. The saturation magnetization of the ferrofluid is about 10 mT and the dielectric number is about 75. The magnetic nanoparticles are coated with an unknown anionic surfactant which serves as a protective layer [26] and prevents particle aggregation [27]. The interfacial tension between the ferrofluid and the silicone oil was measured using a commercial tensiometer (TVT-2, Lauda) and is approximately 25.33 mN m^{-1}.

C. Experimental setup and procedure

The schematic of the experimental setup is shown in Fig. 3. First, the uniform magnetic field is generated using a coil with 350 turns assembled around a C-shaped iron core [28]. A separation gap of 26 mm ensures that the generated magnetic field is homogeneous and uniform. Next, the microfluidic devices are positioned in the middle of the gap. For the flow-focusing device, the channel of the dispersed phase is

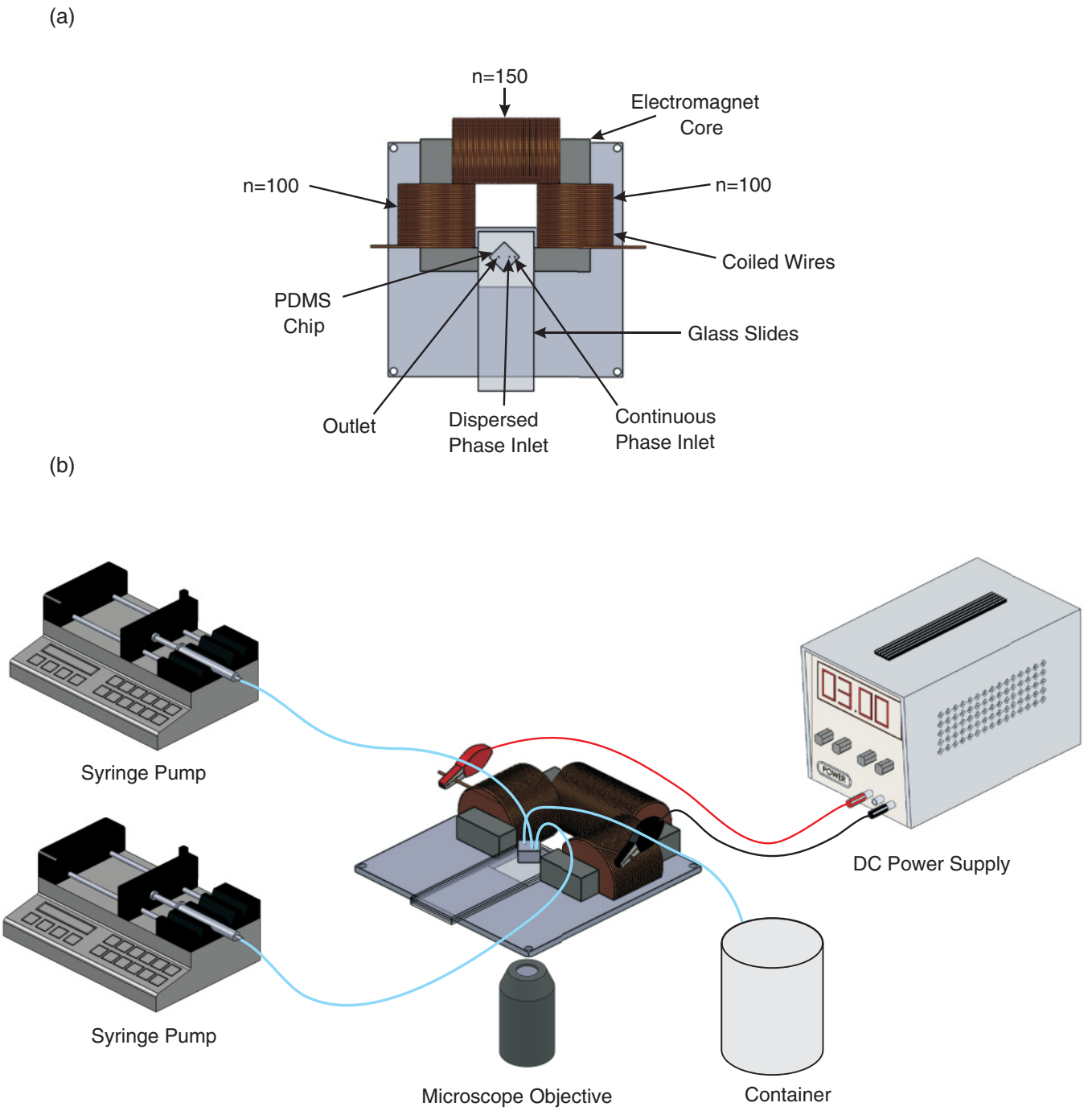

FIG. 3. (Color online) Schematic of the experimental setup (not drawn to scale): (a) top view and details of the electromagnet and (b) experimental setup.

aligned parallel to the magnetic field. For the T-junction device, the channel of the dispersed phase is aligned perpendicular to the magnetic field. During the formation process of the emulsion, the direction of the magnetic field is parallel to the fluid motion in both cases to ensure a fair comparison. Figure 4 shows the measured magnetic field strength at different position relative to the midpoint of the dispersed phase channel in the microfluidic devices. The result shows and confirms the uniformity of the magnetic field within the region of emulsion formation. A first order fit for the measured values depicts a linear straight line with negligible gradient. The magnetic flux densities were measured using a commercial gaussmeter (GM05, Hirst) with an accuracy of $\pm 1\%$. A dc power source (GPS-3030DD, Instek) was used to vary the magnitudes of the magnetic flux density by changing the applied electric current. An inverted microscope (TE 2000, Nikon) and a high-speed camera (APX RS, Photron) were used to capture the droplet formation process. Two syringe pumps (KDS 250, KDS Scientific) were used to deliver the fluids into the microfluidic devices at fixed flow rates separately.

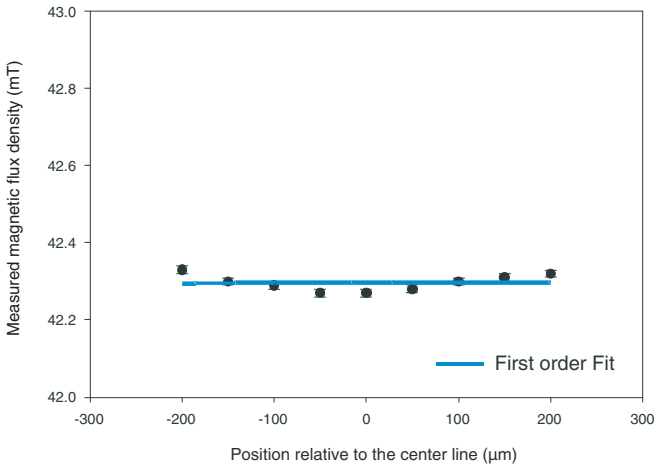

FIG. 4. (Color online) Measured magnetic flux density as a function of position relative to the centerline. The magnetic field is generated using a constant current of 3 A. The centerline represents the midpoint in the dispersed phase channel. A positive distance indicates the upstream and a negative position indicates the downstream position. The position is adjusted using a micropositioner.

The experiments were conducted by fixing the flow rates of both the dispersed and continuous phases and varying the magnetic flux density. Three different sets of flow rates with the same flow rate ratio were tested in the experiments. As silicone oil results in slight swelling of PDMS [29], the fluids were allowed to flow for 20 min before the collection of the images. This measure minimized the structural change within the microfluidic devices and negligible changes were seen within the experimental time frame. Images of the emulsion formation process were acquired at a rate of 1000 frames per second. The sizes of 20 ferrofluid emulsions produced at each interval were then evaluated using customized image processing software (MATLAB, MathWorks). The error bars in Figs. 5 and 8 depicts the standard deviation obtained for each point. The ferrofluid emulsions produced are monodispersed with a polydispersity (defined as the standard deviation of the droplet size divided by the average droplet size) of less than 5%. The magnetic flux density of the electromagnet is varied by changing the supplied current at regular intervals of 0.5 A. A stabilization time of 15 min was also used at each interval.

III. RESULTS AND DISCUSSIONS

A. Flow-focusing configuration

Figure 5(a) shows the diameter of the ferrofluid emulsions formed as a function of magnetic flux density in the flow-focusing geometry. In the absence of the magnetic field, the ferrofluid emulsions are formed in the "geometry-controlled" or "squeezing" regime [21]. The ferrofluid emulsions produced in this regime are highly monodispersed. In each ferrofluid emulsion formation process, the "finger" of the dispersed fluid progresses sequentially into the orifice. As the ferrofluid tip advances, it first increases in size and then evolves into a conical shape. This process limits the flow of the outer fluids and thus results in the change in shape for the dispersed finger. As the dispersed finger blocks the flow of the outer fluids, the

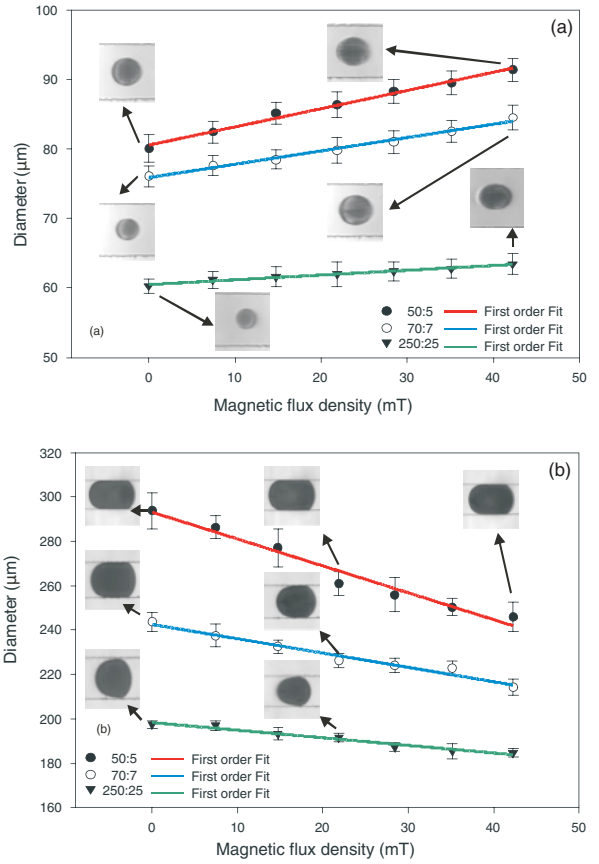

FIG. 5. (Color online) Size of ferrofluid emulsions as a function of magnetic flux density: (a) flow-focusing configuration and (b) T-junction configuration. Each symbol represents the flow rates of the CP:DP in μl h^{-1}. Each colored line represents different fixed flow rates.

upstream pressure builds up gradually. The dispersed finger then elongates and changes the curvature of the neck [30]. Thinning of the neck occurs as the upstream pressure increases. A ferrofluid droplet is formed when the capillary pressure balances with the viscous forces, which then "pinches" off the dispersed neck to form the droplet. After the formation, the dispersed finger retracts to its original position located upstream and returns back to its domical shape. At a fixed flow rate ratio (CP:DP = 10:1), the size of the droplet decreases with the increase of total flow rates [Fig. 5(a)] due to the higher shear rate at higher total flow rates and the less dominant capillary pressure. At a higher total flow rate (CP = 250 μl h^{-1} and DP = 25 μl h^{-1}), the shape of the dispersed finger becomes more conical due to the higher shearing force imposed by the continuous phase. The trends observed throughout the experiments agree with the scaling argument proposed by Garstecki *et al.* [30].

In the presence of a magnetic field, the size of the ferrofluid emulsions produced changes with the applied magnetic flux density. In general, the size increases with the increase of the magnetic flux density; see Fig. 5(a). As the dispersed phase fluid is aligned in the direction of the magnetic field, the magnetic nanoparticles in the dispersed phase align and orient themselves in the direction of the magnetic field [3]. This results in an additional magnetic force which stretches

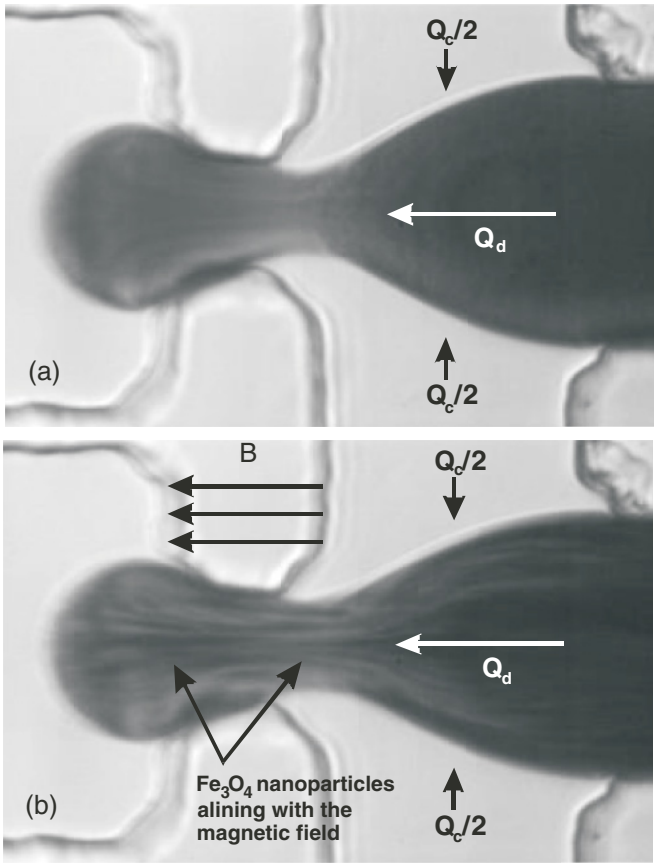

FIG. 6. Alignments of the clustered magnetic nanoparticles in the direction of the magnetic field. In both cases, the flow rates are fixed at 50:5 (CP:DP in μl h^{-1}): (a) without magnetic field and (b) at magnetic flux density of 42.3 mT.

the fluid finger and also induces internal secondary flow. Hence, this delays the thinning process of the neck and consequently the breakup of the droplet. Details of the effect of the magnetic field on the formation process in a flow-focusing configuration were investigated numerically by our group [31,32]. In addition, other factors such as the local change of magnetic-induced changes to the local viscosity [33] and changes in interfacial slips [34] due to the presence of the nanoparticles may also contribute to the changes. Figure 6 depicts the movement of the clustered magnetic nanoparticles along the magnetic field within the dispersed phase. Because the magnetic nanoparticles are not stable under a magnetic field, they tend to form into clusters which can then be seen under the microscope. The experimental results also suggested that these changes are affected by the total flow rate [Fig. 5(a)]. At a higher total flow rate, the change in size of the ferrofluid emulsions at a stronger magnetic field is less prominent and significant. At a higher total flow rate, the dependence on the change in dispersed fluid flow rates is smaller. The first order fits obtained in the experimental results also show a decrease in gradient at higher total flow rates.

B. T-junction configuration

Figure 5(b) shows the diameter of ferrofluid emulsions as a function of magnetic flux density at the T-junction configuration. In the absence of the magnetic field, the ferrofluid emulsions are formed in the same "geometry controlled" or "squeezing" regime. However, under the same flow rates, the sizes of the ferrofluid droplets formed were bigger than the one formed in the flow-focusing configuration, because the dispersed phase fluid is not confined by the orifice [21] which limits the size of the emulsions. In the T-junction geometry, the confinement of the dispersed phase fluid is smaller due to a larger separation distance between the channel of the dispersed phase and the channel of the continuous phase. The size of the orifice in the flow-focusing geometry is about 50 μm and the size of the separation distance in the T junction is about 150 μm. The emulsion formation process in the T junction is also different compared to the flow-focusing configuration. In the T-junction configuration, the ferrofluid droplets are formed via a two-stage growth process [35,36]. First, the dispersed phase fluid gradually extrudes into the continuous-phase channel and occupies the full width of the continuous-phase channel. The obstruction caused by the dispersed fluid also blocks the flow of the continuous-phase fluid, which increases the upstream pressure. The emulsion then grows in size, while reducing the neck of the dispersed phase. The upstream pressure then pinches off the dispersed neck and the emulsion is formed when the dispersed phase fluid cannot withstand the upstream pressure. At a fixed flow rate ratio (CP:DP = 10:1), the sizes of the emulsions produced also change with the change in total flow rate. A smaller ferrofluid emulsion is formed when the total flow rate increases, due to the higher shear rate and lower dependence of capillary pressure at higher flow rates. Compared to the flow-focusing configuration, the change in total flow rates for the T-junction configuration has a greater effect on the size of the formed

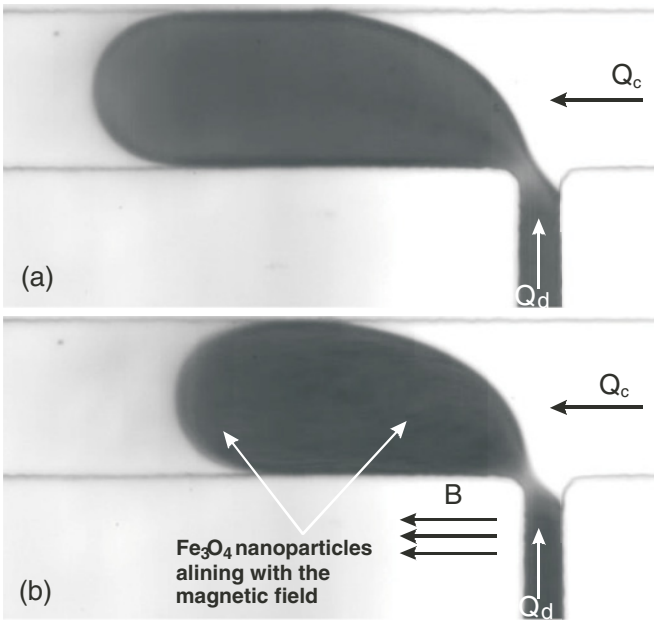

FIG. 7. Alignment of the clustered magnetic nanoparticles in the direction of the magnetic field. In both cases, the flow rates are fixed at 50:5 (CP:DP in μl h^{-1}): (a) without magnetic field and (b) at magnetic flux density of 42.3 mT.

ferrofluid droplets. A greater change in the size of the droplet is observed when the total flow rate increases (Fig. 5).

In the presence of a magnetic field, the size of the ferrofluid emulsions also changes with the applied magnetic flux density. However, in contrast to the flow-focusing geometry, the size of the ferrofluid emulsions produced at the T junction decreases with the increase of the magnetic flux density. This difference in behavior is mainly caused by the orientation of the magnetic field relative to the flow of the ferrofluid. In the flow-focusing configuration, the extruding dispersed phase fluid is parallel to the orientation of the magnetic field. This results in the elongation of the dispersed finger as the ferrofluid aligns itself with the magnetic field, which then delays the emulsion breakup process. However, in the T-junction configuration, the extruding dispersed-phase fluid is perpendicular to the orientation of the magnetic field. As the ferrofluid aligns itself with the direction of the magnetic field, this motion accelerates the thinning process of the neck and causes the droplet to break up earlier as compared to the case without the magnetic field. Figure 7 illustrates the alignments of the clustered magnetic nanoparticles in the direction of the magnetic field in the T-junction configuration. At higher total flow rates, the change in size of the ferrofluid emulsions at higher magnetic flux density is also less prominent. This phenomenon is similar to the one observed in the flow-focusing experiments.

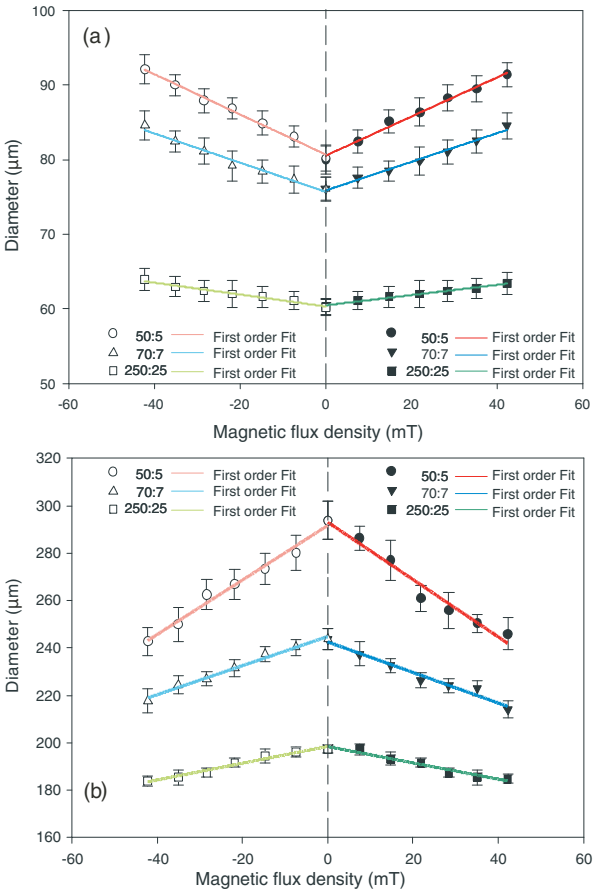

FIG. 8. (Color online) Effect of the polarity of the magnetic field. Each colored line represents different fixed flow rates used. The dark colored lines represent the ferrofluid emulsions formed using a positive magnetic flux density. The light colored lines represent the ferrofluid emulsion formed using a negative magnetic flux density. Each symbol represents the flow rates used in μl h^{-1} (a) using the flow-focusing geometry and (b) using the T-junction geometry.

C. Effect of magnetic polarity

In order to investigate the effect of the magnetic polarity on the size of ferrofluid emulsions produced, the experiments reported above were repeated with a change in the direction of the electrical current. This change in direction of the current induced a change in the polarity of the uniform magnetic field. Figure 8 shows the effect of the magnetic polarity in both flow-focusing and T-junction configurations. Surprisingly, when the direction of the magnetic field is reversed, the trends obtained for the size of the ferrofluid droplets are similar in all cases. This phenomenon suggests that the direction of the magnetic polarity has little or no obvious influence on the size of the ferrofluid emulsion produced in microfluidic devices. This is because, unlike in the previous cases where the orientation of the magnetic field with the dispersed-phase fluid changes from parallel to perpendicular (Fig. 5), the magnetic polarity does not change the alignment direction in the magnetic nanoparticles. In opposite magnetic polarities, the magnetic nanoparticles still align themselves parallel to the magnetic field lines. Hence, as a result, little or no change in seen in the size of the ferrofluid emulsions produced.

IV. CONCLUSIONS

In this study, we introduced a method to produce and actively manipulate the size of the ferrofluid emulsions produced using simple microfluidic devices. Unlike in our previous work, this method offers a flexible and reliable method to control the size of the ferrofluid emulsion produced using simple microfluidic devices. From the experimental results, the following conclusions can be drawn. First, the size of the ferrofluid emulsions formed was found to change with the change in the flow rates, and the orientation and strength of the magnetic field. This demonstrates and confirms that the concept can be used to effectively manipulate the size of the ferrofluid emulsions produced in microfluidic devices. Second, in the flow-focusing configuration, the size of the ferrofluid emulsions produced increases with the increase in magnetic flux density, because the dispersed fluid is parallel to the direction of the magnetic fields. At higher total flow rates (CP:DP = 70:7 and 250:25, CP:DP in μl h^{-1}), the effect is less prominent due to a lower dependence on the changes in the dispersed flow rate. Third, in the T-junction configuration, the size of the ferrofluid emulsions produced decreases with the increase in magnetic flux density, because the dispersed fluid is aligned perpendicularly to the magnetic field. At higher flow rates (CP:DP = 70:7 and 250:25, CP:DP in μl h^{-1}), the effect is also less prominent. Fourth, the effect of the magnetic polarity was found to have no influence on the size of the ferrofluid emulsions produced in both flow-focusing and T-junction geometry, because the direction of the magnetic polarity does not change the alignments of the magnetic nanoparticles with the magnetic field. Finally, this unique method, proposed to actively manipulate the size of

the ferrofluid emulsions formed, may be a simple alternative adopted to solve multiple complex problems faced by many fellow researchers in different fields. This work also opens up exciting opportunities for the use of monodispersed ferrofluid emulsions.

ACKNOWLEDGMENTS

We gratefully acknowledge the insightfully discussions held with Dr. Jean-Christophe Baret and Dr. Benoit Semin from the Max-Planck Institute for Dynamics and Self-organization.

[1] S. S. Nair, J. Thomas, C. S. Suchand Sandeep, M. R. Anantharaman, and R. Philip, Appl. Phys. Lett. **92**, 171908 (2008).
[2] C. Scherer and A. M. Figueiredo Neto, Braz. J. Phys. **35**, 718 (2005).
[3] K. Raj and R. J. Boulton, Mater. Des. **8**, 233 (1987).
[4] L. M. Pop, J. Hilljegerdes, S. Odenbach, and A. Wiedenmann, Appl. Organomet. Chem. **18**, 523 (2004).
[5] S. Odenbach, Colloids Surf. A **217**, 171 (2003).
[6] K. Raj and R. Moskowitz, J. Magn. Magn. Mater. **85**, 233 (1990).
[7] R. L. Bailey, J. Magn. Magn. Mater. **39**, 178 (1983).
[8] K. Raj, B. Moskowitz, and R. Casciari, J. Magn. Magn. Mater. **149**, 174 (1995).
[9] R. Ganguly, A. P. Gaind, S. Sen, and I. K. Puri, J. Magn. Magn. Mater. **289**, 331 (2005).
[10] E. K. Ruuge and A. N. Rusetski, J. Magn. Magn. Mater. **122**, 335 (1993).
[11] A. N. Rusetski and E. K. Ruuge, J. Magn. Magn. Mater. **85**, 299 (1990).
[12] A. S. Lübbe, C. Alexiou, and C. Bergemann, J. Surg. Res. **95**, 200 (2001).
[13] A. G. Boudouvis, J. L. Puchalla, L. E. Scriven, and R. E. Rosensweig, J. Magn. Magn. Mater. **65**, 307 (1987).
[14] V. S. Mendelev and A. O. Ivanov, Phys. Rev. E **70**, 051502 (2004).
[15] M. Ivey, J. Liu, Y. Zhu, and S. Cutillas, Phys. Rev. E **63**, 011403 (2000).
[16] F. Montagne, O. Mondain-Monval, C. Pichot, H. Mozzanega, and A. Elassari, J. Magn. Magn. Mater. **250**, 302 (2002).
[17] Y. Sun, Y. C. Kwok, and N. T. Nguyen, Lab Chip **7**, 1012 (2007).
[18] A. Hatch, A. E. Kamholz, G. Holman, P. Yager, and K. F. Böhringer, J. Microelectromech. Syst. **10**, 215 (2001).
[19] J. Bibette, J. Magn. Magn. Mater. **122**, 37 (1993).
[20] T. Thorsen, R. W. Roberts, F. H. Arnold, and S. R. Quake, Phys. Rev. Lett. **86**, 4163 (2001).
[21] N. T. Nguyen, T. H. Ting, Y. F. Yap, T. N. Wong, J. C. K. Chai, W. L. Ong, J. L. Zhou, S. H. Tan, and L. Yobas, Appl. Phys. Lett. **91**, 084102 (2007).
[22] T. Nisisako, T. Torii, and T. Higuchi, Lab Chip **2**, 24 (2002).
[23] J. H. Xu, S. W. Li, J. Tan, Y. J. Wang, and G. S. Luo, Langmuir **22**, 7943 (2006).
[24] S. Tan, N. Nguyen, L. Yobas, and T. Gang, J. Micromech. Microeng. **20**, 045004 (2010).
[25] D. C. Duffy, J. C. McDonald, O. J. A. Schueller, and G. M. Whitesides, Anal. Chem. **70**, 2280 (1998).
[26] X. R. Qu, S. C. Lü, S. F. Fu, and Q. Y. Meng, Key Eng. Mater. **428–429**, 533 (2010).
[27] N. Pamme, Lab Chip **6**, 24 (2010).
[28] C. Ogawa, Y. Masubuchi, J. I. Takimoto, and K. Koyama, Int. J. Mod. Phys. B **15**, 859 (2001).
[29] M. He, J. Kuo, and D. Chiu, Langmuir **22**, 6408 (2006).
[30] P. Garstecki, H. A. Stone, and G. M. Whitesides, Phys. Rev. Lett. **94**, 164501 (2005).
[31] J. Liu, S. H. Tan, Y. F. Yap, M. Y. Ng, and N. T. Nguyen, Microfluid. Nanofluid. **11**, 177 (2011).
[32] J. Liu, Y. F. Yap, and N. T. Nguyen, Phys. Fluids **23**, 072008 (2011).
[33] C. Flament, S. Lacis, J.-C. Bacri, A. Cebers, S. Neveu, and R. Perzynski, Phys. Rev. E **53**, 4801 (1996).
[34] S. M. S. Murshed, S. H. Tan, N. T. Nguyen, T. N. Wong, and L. Yobas, Microfluid. Nanofluid. **6**, 253 (2009).
[35] H. Liu and Y. Zhang, J. Appl. Phys. **106**, 034906 (2009).
[36] M. De Menech, P. Garstecki, F. Jousse, and H. A. Stone, J. Fluid Mech. **595**, 141 (2008).